

Genome-wide analysis of histone modifications by ChIP-chip to identify silenced genes in gastric cancer

XINJIANG ZHU^{1,2}, JIAN LIU¹, XIAOYANG XU¹, CHUNDONG ZHANG¹ and DONGQIU DAI¹

¹Department of Gastrointestinal Surgery, The Fourth Affiliated Hospital, China Medical University, Shenyang, Liaoning 110032; ²Internal Medicine, Liaoning Province Tumor Hospital, Shenyang, Liaoning 110042, P.R. China

Received October 26, 2014; Accepted January 30, 2015

DOI: 10.3892/or.2015.3824

Abstract. The present study aimed to identify novel histone modification markers in gastric cancer (GC) by chromatin immunoprecipitation microarray (ChIP-chip) analysis and to determine whether these markers were able to discriminate between normal and GC cells. We also tested for correlations with DNA methylation. We probed a human CpG island microarray with DNA from a GC cell line (MKN45) by chromatin immunoprecipitation (ChIP). ChIP-reverse-transcriptase quantitative polymerase chain reaction PCR (RT-qPCR) was used to validate the microarray results. Additionally, mRNA expression levels and the DNA methylation of potential target genes were evaluated by RT-qPCR and methylation-specific PCR (MSP). The results showed that 134 genes exhibited the highest signal-to-noise ratio of H3-K9 trimethylation over acetylation and 46 genes exhibited the highest signal-to-noise ratio of H3-K9 trimethylation over H3-K4 trimethylation in MKN45 cells. The ChIP-qPCR results agreed with those obtained from the ChIP-chip analysis. Aberrant DNA methylation status and mRNA expression levels were also identified for selected genes (*PSD*, *SMARCC1* and *Vps37A*) in the GC cell lines. The results suggest that CpG island microarray coupled with ChIP (ChIP-chip) can identify novel targets of gene silencing in GC. Additionally, ChIP-chip is the best approach for assessing the genome-wide status of epigenetic regulation, which may allow for a broader genomic understanding compared to the knowledge that has been accumulated from single-gene studies.

Introduction

Gastric cancer (GC) is one of the most common malignancies and is the second and third leading cause of cancer-related mortality in men and women, respectively, worldwide. Compared to other malignant types of cancer, the incidence

and mortality of GC ranks first in China; where the cases account for 42% of all GC cases worldwide (1). Most patients are diagnosed at an advanced stage, thus GC continues to be a highly aggressive malignancy that is associated with poor prognosis and a low survival rate. Therefore, additional studies are needed to explore the molecular pathophysiology of GC.

Mounting evidence has indicated that epigenetic alterations play a key role in the occurrence and development of GC (2,3). These epigenetic alterations, such as DNA and histone methylation, provide an alternative pathway for gene silencing that is distinct from gene mutation and deletion. Tumor-suppressor gene (TSG) silencing associated with DNA methylation in cancer is accompanied by abnormal histone modifications (4,5). Histone modifications, which have been recently recognized to generate a 'histone code' that affects chromatin structure and gene expression, also play an important role in the establishment of gene silencing during tumorigenesis (6). Histone lysine methylation and acetylation, which are two of the best-studied histone modifications, are involved in many biological processes, including gene activation and silencing, DNA methylation, X-chromosome inactivation, DNA repair and cell cycle control (7). H3-K9 acetylation is known to be associated with active transcription, whereas H3-K9 trimethylation has been connected with repressed transcription (8). Furthermore, H3-K4 trimethylation has been detected at active genes and is thought to promote gene expression. Histone acetylation and methylation are likely to act cooperatively to regulate gene transcription.

In the post-genomic era, high-throughput technologies have made it possible to analyze the chromatin structure at the genomic scale in cancer cells. Chromatin immunoprecipitation coupled with microarray (ChIP-chip) has been used by investigators to conduct genome-wide analyses (9,10). In the recent study, we used the ChIP-chip technique to characterize inactive genes in GC, with an aim to identify the targets of genes controlled by histone modifications. We also examined the relevance of histone modifications and DNA methylation for these genes. The results showed that the histone modifications and DNA methylation study acted cooperatively to affect gene expression in GC.

Materials and methods

Cell culture and treatment with epigenetic agents. The human MKN45, AGS, BGC823 and SGC7901 GC cell lines

Correspondence to: Professor Dongqiu Dai, Department of Gastrointestinal Surgery and Cancer Center, The Fourth Affiliated Hospital of China Medical University, 4 Chongshan East Road, Shenyang, Liaoning 110032, P.R. China
E-mail: daidq63@163.com

Key words: ChIP-chip, tumor-suppressor genes, gastric carcinoma, histone modification, DNA methylation

Table I. ChIP-qPCR primers used for validation of the ChIP-chip data.

Gene	Primer sequence (5→3)	Annealing temperature (°C)	Size (bp)
<i>PSD</i>	F: GACTGGCTTCTGTCGTCCTC R: GGCAGACAGTAAGAGCCTGG	60	190
<i>NLK</i>	F: TGTCTATTTGGCCCAGGTTC R: AAAGGCAGAGTTTGGCTTGA	59	201
<i>SMARCC1</i>	F: TTCAAGCAATTCTCCTGCCT R: CGCCTGTAATCCCAACTT	59	183
<i>Vps37A</i>	F: CAGTGC GAAGGTGCTGATAA R: ACGATGAACCTGAGAGGGTG	60	280

F, forward primer; R, reverse primer; ChIP-chip, chromatin immunoprecipitation microarray; qPCR, quantitative polymerase chain reaction.

were obtained from the Institute of Biochemistry and Cell Biology, Chinese Academy of Sciences (Shanghai, China). The immortalized GES1 normal gastric cell line was obtained from the Oncology Institute of China Medical University. The cells were cultured in RPMI-1640 medium supplemented with 10% fetal bovine serum (Gibco-BRL, Grand Island, NY, USA) and incubated at 37°C in a humidified 5% CO₂ atmosphere. The four GC lines were incubated in culture media with 5 μM of the DNA methyltransferase (DNMT) inhibitor 5-aza-2'-deoxycytidine (DAC) for 3 days, and 0.3 μM of the histone deacetylase (HDAC) inhibitor trichostatin A (TSA) (both from Sigma-Aldrich, St. Louis, MO, USA) for 1 day. The time, dose and sequence of DAC and/or TSA were based on previous studies (11,12).

Chromatin immunoprecipitation (ChIP) assay. Five million cells were crosslinked with 1% formaldehyde for 10 min at 37°C, and then 0.125 M of glycine was added to stop the crosslinking. After washing with ice-cold PBS, the cell pellets were resuspended in lysis buffer, and sonicated to generate 200 to 1,000-bp DNA fragments. The lysate was then divided into three fractions. The first lysate was precipitated using antibodies against Lys-9 trimethylated histone H3 (05-1242), Lys-9 acetylated histone H3 (07-352) and Lys-4 trimethylated histone H3 (07-472) (all from Millipore, Billerica, MA, USA) at 4°C overnight. The second lysate was incubated with normal rabbit IgG (Santa Cruz Biotechnology Inc., Santa Cruz, CA, USA) as a negative control. The third lysate was used as an input control. Protein G-Sepharose beads were added to collect the immunoprecipitated complexes and left them to incubate for 1 h at 4°C. After washing, the beads were treated with RNase (50 mg/ml) for 30 min at 37°C and then proteinase K overnight. The crosslinks were then reversed by heating the sample at 65°C for 6 h. DNA was extracted by the phenol/chloroform method, ethanol precipitated, and resuspended in 20 μl water.

ChIP-chip. Immunoaffinity-enriched DNA fragments (IP) and input samples were amplified using a Whole Genome Amplification kit (Sigma-Aldrich). Input and IP samples were labeled in separate reactions with Cy3 and Cy5, respectively and were co-hybridized to a Human 3 x 720K RefSeq Promoter Array (NimbleGen, Madison, WI, USA), containing 22,542 human promoter regions that cover a range from

-3,200 to +800 bp, relative to the transcription start site. The hybridized microarray slides were scanned using a GenePix 4000B scanner (Axon Instruments, Foster City, CA, USA). Data were extracted using NimbleScan software. From the normalized log₂-ratio data, a permutation-based peak finding algorithm provided by NimbleScan version 2.3 (NimbleGen) was used to detect peaks that represented significant positive enrichment. To detect the peaks for histone modification, only the false discovery rate (FDR <0.05) was considered for analysis.

ChIP-qPCR. ChIP was conducted in the same manner as for ChIP-chip. Briefly, immunoaffinity-enriched, input, and negative control DNA were used for PCR. Primers were designed based on the promoter structure of the genes selected for evaluating ChIP-chip data (Table I). PCR products were visualized on a 2.5% agarose gel. For quantification, PCR amplification was performed on an ABI 7700 real-time PCR (Applied Biosystems, Foster City, CA, USA). PCR conditions included an initial denaturation step of 4 min at 95°C, followed by 35 cycles of 5 sec at 95°C, 30 sec at 59°(60°)C and 20 sec at 72°C. Quantitative ChIP-PCR values were normalized against values from a standard curve constructed using input DNA that was extracted for the ChIP experiment. ChIP experiments were repeated three times for each target gene.

RNA extraction and reverse-transcriptase quantitative polymerase chain reaction (RT-qPCR). Total RNA was extracted from cells and tissues with TRIzol reagent (Invitrogen, Carlsbad, CA, USA) according to the manufacturer's instructions. The quality and concentration of RNA were measured by ultraviolet absorbance at 260 and 280 nm (A₂₆₀/A₂₈₀ ratio) and checked by agarose gel electrophoresis individually. Total RNA was reverse transcribed into cDNA using an Expand Reverse Transcriptase kit (Takara, Dalian, China). Expression of PSD mRNA was detected using qPCR under the following conditions: 95°C for 30 sec, 35 cycles of 95°C for 5 sec and 60°C for 30 sec. The reaction mixture contained 12.5 μl SYBR-Green (Takara), 1 μl of each primer, 2 μl cDNA, and 8.5 μl diethylpyrocarbonate (DEPC)-treated water. The PCR primers used for each gene in this analysis are shown in Table II. Negative control used DEPC-treated water to replace cDNA templates for each PCR. The PSD level was expressed

Table II. Primers used for RT-qPCR analysis.

Gene	Primer sequence (5→3)	Annealing temperature (°C)	Size (bp)
<i>PSD</i>	F: CTGGGCAAGAACAATGACTTC R: GAGGACAGGGCTTCAGGATT	58	140
<i>SMARCC1</i>	F: TGAACGGGAAGCTCACTGG R: TCCACCACCCTGTTGCTGTA	59	249
<i>Vps37A</i>	F: CGCCAGCATCCACCACG R: TTGAGTTTGTGAATGAC	60	283
<i>GAPDH</i>	F: CATGAGAAGTATGACAACAGCCT R: AGTCCTTCCACGATACCAAAGT	60	257

F, forward primer; R, reverse primer; RT-PCR, reverse-transcriptase quantitative polymerase chain reaction.

Table III. Primers used for MSP analysis.

Gene	Primer sequence (5→3)	Annealing temperature (°C)	Size (bp)
<i>PSD-M</i>	F: GTTGTAGGGAAGCGGTTTC R: CGACCACGAAAAAAAACC	55	150
<i>PSD-U</i>	F: AGGGTTGTAGGGAAGTGTTT R: CAACCACAAAAAAAACCTA	55	151
<i>SMARCC1-M</i>	F: GGATTACGAGGTTAGGAGATC R: CGACTCACTACAACTCCG	56	180
<i>SMARCC1-U</i>	F: GGATTATGAGGTTAGGAGATT R: CAACTCACTACAACTCCA	56	181
<i>Vps37A-M</i>	F: TAGAGATAGTATTCGGCGGC R: TCAAAACGTACGAAAAACGA	59	130
<i>Vps37A-U</i>	F: TTATAGAGATAGTATTTGGTG R: TCAAAACATACAAAAACAAC	59	131

F, forward primer; R, reverse primer; MSP, methylation-specific PCR.

as C_t after normalization to the levels of GAPDH mRNA. The experiment was performed in triplicate.

Methylation-specific PCR (MSP). Genomic DNA was extracted from cells with phenolchloroform-isoamyl alcohol and collected by ethanol precipitation. Genomic DNA (2 μ g) was treated with NaOH (2 M) at 42°C for 20 min. After denaturation, the DNA was incubated with hydroquinone and sodium bisulfate at 54°C for 16 h in the dark. DNA was purified using a DNA Cleanup kit (Promega, Madison, WI, USA), followed by incubation with 3 M NaOH at 37°C for 15 min, and precipitation with ammonium acetate and 100% ethanol at -20°C overnight. The following day, DNA was washed with 70% ethanol, and dissolved in 15 μ l TE buffer. The primers used for MSP were located in the promoter region of the genes (Table III). Peripheral blood cell DNA from healthy adults treated with SssI methyltransferase (New England Biolabs, Ipswich, MA, USA) and untreated DNA were used as positive and negative controls, respectively. PCR products were separated by electrophoresis on 2% agarose gels, and quantified using the Fluor Chen 2.0 system.

Statistical analysis. Statistical analyses were performed using SPSS version 17.0 (SPSS, Chicago, IL, USA). Quantitative data are shown as mean values \pm SD. Statistical analyses were performed using the independent sample t-test. $P < 0.05$ was considered statistically significant.

Results

Genome-wide analysis of histone modifications by ChIP-chip. TSG inactivation resulting from higher H3-K9 trimethylation, lower H3-K9 acetylation and H3-K4 trimethylation has been reported to be involved in carcinogenesis. We aimed to identify genes that underwent similar histone modifications in GC cells. We used a two-step strategy to analyze the data. First, we selected 134 candidate genes that showed a high ratio of H3-K9 trimethylation over acetylation (H3-K9Me3/H3-K9Ac > 2.0). The selected 20 genes with a high ratio of H3-K9 trimethylation over H3-K9 acetylation are presented in Table IV. We then analyzed 46 candidate genes that showed a high ratio of H3-K9 trimethylation over H3-K4 trimethylation (H3-K9Me3/H3-K4Me3 > 2.0). The selected 20 genes with a

Table IV. Twenty genes showing a high ratio of H3-K9 trimethylation over acetylation (H3-K9 Me₃/H3-K9Ac >2.0), identified by ChIP-CpG microarray.

Accession no.	Location	Gene symbol	Description	Fold-change
NM_170743	Chr 1: 24386073-24386599	<i>IL28RA</i>	Interleukin 28 receptor, α (interferon, λ receptor)	4.14
NM_001145442	Chr 14: 19090441-19091120	<i>POTEM</i>	POTE ankyrin domain family, member M	3.58
NM_021080	Chr 1: 58488062-58488534	<i>DABI</i>	Disabled homolog 1 (<i>Drosophila</i>)	3.19
NM_005186	Chr 11: 64705434-64705961	<i>CAPN1</i>	Calpain 1, (μ /I) large subunit	3.08
NM_014588	Chr 2: 25010707-25011384	<i>VSX1</i>	Visual system homeobox 1	2.99
NM_001145152 ^a	Chr 8: 17149196-17149585	<i>Vps37A</i>	Vacuolar protein sorting 37 homolog A	2.98
NM_001079526	Chr 2: 213724263-213724861	<i>IKZF2</i>	IKAROS family zinc finger 2	2.97
NM_153456	Chr 13: 95541348-95541914	<i>HS6ST3</i>	Heparan sulfate 6-O-sulfotransferase 3	2.96
NM_201269	Chr 1: 91259477-91260224	<i>ZNF644</i>	Zinc finger protein 644	2.95
NM_032991	Chr 4: 185807070-185807632	<i>CASP3</i>	Caspase-3, apoptosis-related cysteine peptidase	2.94
NM_138785	Chr 6: 149928999-149929638	<i>C6orf72</i>	Chromosome 6 open reading frame 72	2.94
NM_020680	Chr 11:65049471-65049926	<i>SCYL1</i>	SCY1-like 1 (<i>S. cerevisiae</i>)	2.92
NM_024907	Chr 19: 44158164-44158927	<i>FBXO17</i>	F-box protein 17	2.92
NM_014718	Chr 12: 7173825-7174446	<i>CLSTN3</i>	Calsyntenin 3	2.92
NM_017924	Chr 14: 22633202-22634021	<i>C14orf119</i>	Chromosome 14 open reading frame 119	2.92
NM_022898	Chr 14: 98807632-98808446	<i>BCL11B</i>	B-cell CLL/lymphoma 11B (zinc finger protein)	2.90
NM_014229	Chr 22: 10832813-10833404	<i>SLC6A11</i>	Solute carrier family 6 member 11	2.90
NM_021255	Chr 14: 55654533-55655026	<i>PELI2</i>	Pellino homolog 2 (<i>Drosophila</i>)	2.89
NM_016231 ^a	Chr 17: 23392754-23393241	<i>NLK</i>	Nemo-like kinase	2.48
NM_003074 ^a	Chr 3: 47798031-47798567	<i>SMARCC1</i>	SWI/SNF-related, matrix-associated, actin-dependent regulator of chromatin, subfamily c, member 1	2.44

^aSelected genes used for validation of the ChIP-chip data. ChIP-chip, chromatin immunoprecipitation microarray; Chr, chromosome.

high ratio of H3-K9 trimethylation over H3-K4 trimethylation are presented in Table V.

Validation for ChIP-chip data. To validate the microarray results, the selected genes, *PSD*, *NLK*, *SMARCC1* and *Vps37A* exhibited a high ratio of H3-K9 trimethylation over acetylation or a high ratio of H3-K9 methylation over H3-K4 trimethylation in the MKN45 cell line. These results were verified by ChIP-qPCR. As shown in Table VI and Fig. 1, qPCR results for the selected candidate genes were consistent with the ChIP-chip data.

Differential mRNA expression in GC cells. Using qRT-PCR to assess the mRNA expression levels of *SMARCC1* and *Vps37A*, we found that *SMARCC1* was downregulated in MKN45 (0.5377 \pm 0.01126), AGS (0.5697 \pm 0.00963), BGC823 (0.3157 \pm 0.0099) and SGC7901 (0.527 \pm 0.0046) cells compared to the normal mucosa cell line, GES-1 (1-fold, as was the control). Of note, the mRNA expression levels of *Vps37A* were similar between GC and GES-1 cells (Fig. 2).

Effects of 5-aza-2'-DAC and TSA on gene re-expression. To determine whether epigenetic agents altered *PSD*, *SMARCC1* and *Vps37A* gene expression levels, we treated MKN45 cells with the DNMT inhibitor DAC, the HDAC inhibitor TSA, or a combined treatment of the two agents. Using RT-qPCR, we found that DAC and TSA had different effects on the expression of these genes in MKN45 cells. DAC alone restored *PSD* expression, whereas TSA had no effect on *PSD* expression. The combined treatment restored *PSD* expression levels similar to those observed after DAC treatment. DAC or TSA alone restored *SMARCC1* expression and the combined treatment with the two agents restored *SMARCC1* expression to a significantly greater degree than the treatment with either agent alone. Treatment with DAC and TSA, alone or in combination, had no significant effect on *Vps37A* expression (Fig. 3).

Expression of the *PSD*, *SMARCC1* and *Vps37A* genes is associated with DNA methylation. To determine whether DNA methylation affected the expression levels of these genes, we assessed their DNA methylation status in MKN45 cell

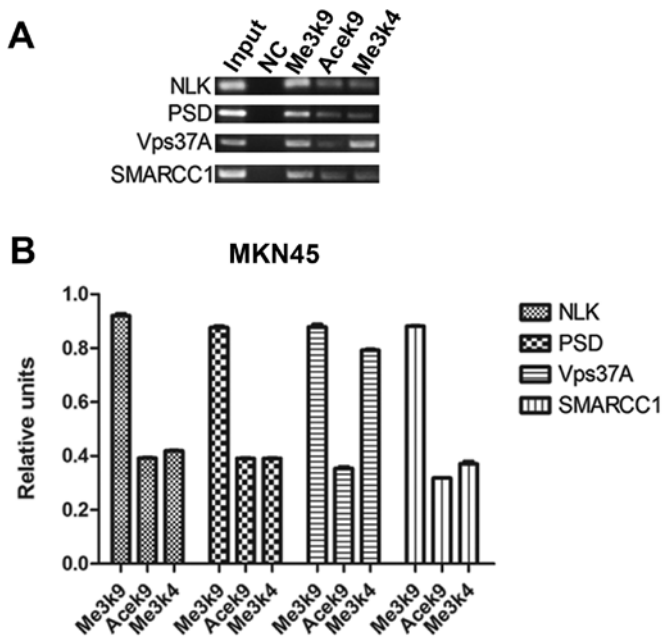


Figure 1. Quantitative polymerase chain reaction verification of ChIP-chip data. (A) Representative graphs of ChIP-qPCR. (B) Quantitative ChIP-PCR experiments were repeated three times. Average precipitate DNA/input DNA ratios shown on the y-axis are the relative values of H3-K9 trimethylation, H3-K9 acetylation and H3-K4 trimethylation at the selected genes promoter region. ChIP-chip, chromatin immunoprecipitation microarray.

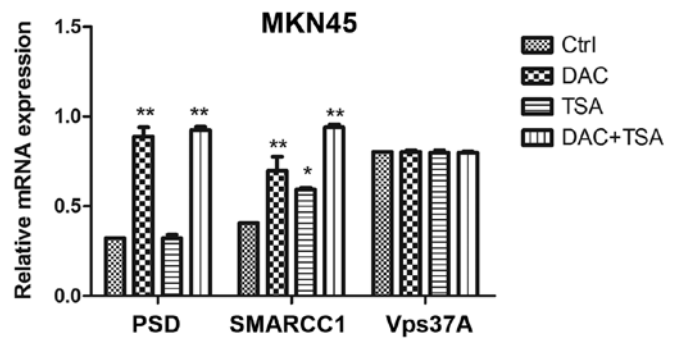


Figure 3. RT-qPCR analysis of the selected genes mRNA expression following treatment with epigenetic agents in MKN45 (* $P < 0.05$, ** $P < 0.01$). RT-qPCR, reverse-transcriptase quantitative polymerase chain reaction PCR.

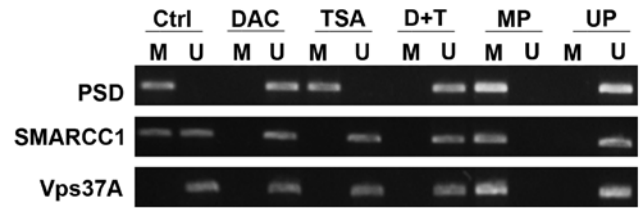


Figure 4. MSP analysis of DNA methylation of the selected genes following treatment with epigenetic agents in MKN45 cells. Lane M indicates the presence of methylated alleles. Lane U indicates the presence of unmethylated alleles. UP, non-methylation positive control; MP, methylation positive control; MSP, methylation-specific PCR.

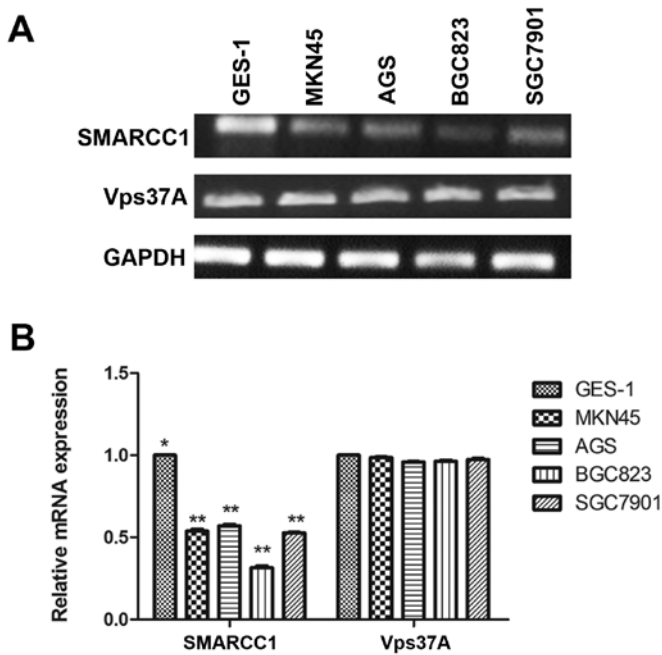


Figure 2. RT-qPCR analysis of the selected genes mRNA expression in MKN45 cells. (A) Representative graphs of RT-PCR assay. (B) RT-qPCR analysis shows mRNA expression of the selected genes in GES1 cells and four different types of GC cell lines (* $P < 0.05$, ** $P < 0.01$). RT-qPCR, reverse-transcriptase quantitative polymerase chain reaction PCR.

lines using MSP. We observed hypermethylation of the PSD promoter, partial methylation of the SMARCC1 promoter, and no methylation of the Vps37A promoter, suggesting that

the methylation status of these gene promoters was partially responsible for the mRNA expression levels. In MKN45 cells, treatment with DAC resulted in demethylation of the PSD and SMARCC1 promoters, and treatment with TSA resulted in demethylation of the SMARCC1 promoter. However, TSA had no effect on the PSD promoter. Treatment with DAC, TSA or both had no effect on the Vps37A promoter (Fig. 4).

Discussion

Epigenetic dysregulation of gene silencing plays a causal role in cancer development and progression. One of the most common epigenetic alterations in cancer results from histone modifications. Modifications of histone tails are thought to specify a code that regulates gene expression (13). The emerging consensus is that high levels of H3-K9 trimethylation, and low levels of H3-K9 acetylation and H3-K4 trimethylation are associated with inactive genes. Previous studies of histone modifications were limited to single-gene disruption (?). However, accumulating evidence shows that multiple genes may simultaneously be involved in gastric tumorigenesis. Advances in high-throughput techniques have enabled the development of ChIP analysis combined with DNA microarray (ChIP-chip), making it possible to profile and quantify the expression of thousands of genes simultaneously. This new high-throughput method has been widely used in epigenetics (14-17). Thus, in the present study, we used a ChIP-chip strategy to explore gene silencing events associated with higher levels of H3-K9 trimethylation, and lower levels of H3-K9 acetylation and H3-K4 trimethylation. These genes

Table V. Twenty selected genes showing a high ratio of H3-K9 trimethylation over H3-K4 trimethylation (H3-K9 Me3/H3-K4Me3 >2.0), identified by ChIP-CpG microarray.

Accession no.	Location	Gene symbol	Description	Fold-change
NM_002226	Chr14: 104705881-104706590	<i>JAG2</i>	Jagged 2	3.02
NM_001127899	ChrX: 49573893-49574453	<i>CLCN5</i>	Chloride channel 5	2.96
NM_032560	Chr14: 91045898-91046864	<i>SMEK1</i>	SMEK homolog 1, suppressor of mek1 (<i>Dictyostelium</i>)	2.95
NM_015500	Chr21: 42246382-42246894	<i>C2CD2</i>	C2 calcium-dependent domain containing 2	2.92
NM_003224	Chr20: 61809198-61810017	<i>ARFRP1</i>	ADP-ribosylation factor-related protein 1	2.92
NM_001101314	Chr7: 150128124-150128968	<i>TMEM176B</i>	Transmembrane protein 176B	2.91
NM_080622	Chr20: 61963760-61964422	<i>C20orf135</i>	Chromosome 20 open reading frame 135	2.90
NM_014618	Chr9: 121171512-121171970	<i>DBC1</i>	Deleted in bladder cancer 1	2.90
NM_001006	Chr4: 152239592-152240103	<i>RPS3A</i>	Ribosomal protein S3A	2.86
NM_002779 ^a	Chr10:104167927-104168755	<i>PSD</i>	Pleckstrin and Sec7 domain containing	2.60
NM_001012614	Chr4: 1232543-1233011	<i>CTBP1</i>	C-terminal binding protein 1	2.57
NM_001409	Chr1: 3517795-3518285	<i>MEGF6</i>	Multiple EGF-like-domains 6	2.46
NM_016231 ^a	Chr17: 23392754-23393241	<i>NLK</i>	Nemo-like kinase	2.45
NM_138328	Chr17: 27616688-27617453	<i>RHBDL3</i>	Rhomboid, veinlet-like 3 (<i>Drosophila</i>)	2.39
NM_005923	Chr6: 137155422-137155958	<i>MAP3K5</i>	Mitogen-activated protein kinase 5	2.35
NM_003074 ^a	Chr3: 47798031-47798567	<i>SMARCC1</i>	SWI/SNF-related, matrix-associated, actin-dependent regulator of chromatin, subfamily c, member 1	2.30
NM_014806	Chr9: 35479779-35480211	<i>RUSC2</i>	RUN and SH3 domain containing 2	2.26
NM_015549	Chr14: 64241089-64241538	<i>PLEKHG3</i>	Pleckstrin homology domain containing, family G (with RhoGef domain) member 3	2.22
NM_001083591	Chr10: 11247329-11247847	<i>CELF2</i>	CUGBP, Elav-like family member 2	2.17
NM_001031807	Chr15: 65903316-65904082	<i>SKORI</i>	SKI family transcriptional corepressor 1	2.10

^aSelected genes used for validation of the ChIP-chip data; ChIP-chip, chromatin immunoprecipitation microarray.

Table VI. Results of ChIP-qPCR and ChIP-chip.

Variable	<i>NLK</i>	<i>PSD</i>	<i>Vps37A</i>	<i>SMARCC1</i>
ChIP-qPCR				
H3-K9Me3	0.9204±0.0069	0.8760±0.0049	0.8789±0.009	0.8811±0.0018
H3-K9Ac	0.3924±0.0024	0.3910±0.0015	0.3540±0.0058	0.3176±0.0015
H3-K4Me3	0.4185±0.0015	0.3909±0.0017	0.7920±0.0036	0.3708±0.0091
K9Me3/K9Ac	2.34	2.24	2.48	2.77
K9Me3/K4Me3	2.20	2.24	1.11	2.38
ChIP-chip				
K9Me3/K9Ac	2.48	2.34	2.98	2.44
K9Me3/K4Me3	2.45	2.60	0.97	2.30

ChIP-chip, chromatin immunoprecipitation microarray; qPCR, quantitative polymerase chain reaction.

included TSG, oncogenes, cell adhesion molecules and cycle regulators, and apoptosis-regulating genes. We also used ChIP-qPCR to confirm the microarray data. We selected

four genes with a high ratio of H3-K9 trimethylation over acetylation, or a high ratio of H3-K9 methylation over H3-K4 trimethylation. The *NLK*, *PSD*, *SMARCC1* and *Vps37A* genes

were used to validate the microarray results in the MKN45 cell line, and the result consistency ultimately proved the value of this approach.

Among the candidates identified by ChIP-chip, PSD is a guanine nucleotide exchange factor for ADP-ribosylation factor 6 (ARF6) (18), which regulates the membrane trafficking of small G proteins (19). The PSD allele is located on human chromosome 10q24 and encodes a 71-kDa protein (20). Okada *et al* (21) reported that PSD was more frequently methylated in ulcerative colitis (UC)-associated colorectal cancer tissues than in non-neoplastic UC epithelia. Additionally, PSD mRNA expression levels were positively correlated with the methylation status of PSD. SMARCC1 is a member of the SWI/SNF complex that has been shown to have tumor-suppressive abilities related to cell cycle control (22,23). However, the expression and function of SMARCC1 in tumorigenesis remains unclear. Loss of SMARCC1 expression contributed to tumor development as a consequence of its location on chromosome band 3p21.31, which includes other suspected TSGs, such as *SEM3B* and *FUS1* (24,25). DelBove *et al* (26) indicated that lower levels of SMARCC1 protein expression in an ovarian carcinoma cell line, SKOV3, closely correlated with mutations in exon 24. The human homologue of Vps37A (hVps37A) is located on the short arm of chromosome 8. In this region, 8p22, loss of heterozygosity (LOH) occurs at a high frequency in several human cancers (27). Wittinger *et al* found that hVps37A was significantly downregulated in ovarian cancer and that hVps37A-deficient cells become non-responsive to inhibition by the therapeutic antibody cetuximab (28).

However, the roles of the selected genes in GC have not been investigated. In the present study, as anticipated, there was a low level of SMARCC1 expression in GC cell lines compared to GES-1 cells. Of note, mRNA expression levels of Vps37A in GC cell lines were similar to GES-1 cells. This exception is probably a consequence of other epigenetic modifications associated with transcriptional activation in this gene. DNA methylation is the most widely studied epigenetic event. Recent investigations have indicated that aberrant DNA methylation is associated with GC (29,30). In order to gain a better understanding of these potential exceptions, we characterized DNA methylation. Our data confirmed hypermethylation of the PSD and SMARCC1 promoters, and hypomethylation of the Vps37A promoter. Additionally, epigenetic agents resulted in the demethylation of the PSD and SMARCC1 promoters and reversed PSD and SMARCC1 expression levels. However, there was no obvious change in Vps37A expression levels following treatment with epigenetic modifying agents.

In summary, data from our current study show that microarray profiling coupled with ChIP using anti-H3-K9 trimethylation and acetylation, as well as H3-K4 trimethylation antibodies is a useful approach for identifying target genes silenced by the epigenetic machinery. We also identified epigenetic mechanisms underlying the decreased expression of PSD and SMARCC1: DNA hypermethylation, hypertrimethylation of H3-K9 and hypotrimethylation of H3-K4 in the promoter domain. By contrast, Vps37A expression was mainly affected by DNA methylation, but not by H3-K9 trimethylation, H3-K9 acetylation or H3-K4 trimethylation. These novel

candidate genes are potential biomarkers or future therapeutic targets. Further investigations are needed to clarify the roles of these candidate genes in the development of GC.

Acknowledgements

The present study was supported partly by a grant from the National Natural Science Foundation of China (grant no. 30572162), the Foundation of Liaoning Province Science and Technology Plan Project (grant no. 2013225021) and the Higher Specialized Research Fund for Doctoral Program of the Ministry of Education of China (grant no. 20102104110001).

References

- Jemal A, Bray F, Center MM, Ferlay J, Ward E and Forman D: Global cancer statistics. *CA Cancer J Clin* 61: 69-90, 2011.
- Park YS, Jin MY, Kim YJ, Yook JH, Kim BS and Jang SJ: The global histone modification pattern correlates with cancer recurrence and overall survival in gastric adenocarcinoma. *Ann Surg Oncol* 15: 1968-1976, 2008.
- Meng CF, Zhu XJ, Peng G and Dai DQ: Role of histone modifications and DNA methylation in the regulation of O6-methylguanine-DNA methyltransferase gene expression in human stomach cancer cells. *Cancer Invest* 28: 331-339, 2010.
- Kim M, Jang HR, Kim JH, *et al*: Epigenetic inactivation of protein kinase D1 in gastric cancer and its role in gastric cancer cell migration and invasion. *Carcinogenesis* 29: 629-637, 2008.
- Jung Y, Park J, Bang YJ and Kim TY: Gene silencing of TSPYL5 mediated by aberrant promoter methylation in gastric cancers. *Lab Invest* 88: 153-160, 2008.
- Jones PA and Baylin SB: The fundamental role of epigenetic events in cancer. *Nat Rev Genet* 3: 415-428, 2002.
- Ruthenburg AJ, Allis CD and Wysocka J: Methylation of lysine 4 on histone H3: intricacy of writing and reading a single epigenetic mark. *Mol Cell* 25: 15-30, 2007.
- Fuks F: DNA methylation and histone modifications: teaming up to silence genes. *Curr Opin Genet Dev* 15: 490-495, 2005.
- Kondo Y, Shen L, Cheng AS, *et al*: Gene silencing in cancer by histone H3 lysine 27 trimethylation independent of promoter DNA methylation. *Nat Genet* 40: 741-750, 2008.
- Zha L, Wang Z, Tang W, Zhang N, Liao G and Huang Z: Genome-wide analysis of HMGA2 transcription factor binding sites by ChIP on chip in gastric carcinoma cells. *Mol Cell Biochem* 364: 243-251, 2012.
- Fahrner JA, Eguchi S, Herman JG and Baylin SB: Dependence of histone modifications and gene expression on DNA hypermethylation in cancer. *Cancer Res* 62: 7213-7218, 2002.
- Cameron EE, Bachman KE, Myöhänen S, Herman JG and Baylin SB: Synergy of demethylation and histone deacetylase inhibition in the re-expression of genes silenced in cancer. *Nat Genet* 21: 103-107, 1999.
- Jenuwein T and Allis CD: Translating the histone code. *Science* 293: 1074-1080, 2001.
- Zhang L, Zhong K, Dai Y and Zhou H: Genome-wide analysis of histone H3 lysine 27 trimethylation by ChIP-chip in gastric cancer patients. *J Gastroenterol* 44: 305-312, 2009.
- Wu J, Wang SH, Potter D, Liu JC, Smith LT, Wu YZ, Huang TH and Plass C: Diverse histone modifications on histone 3 lysine 9 and their relation to DNA methylation in specifying gene silencing. *BMC Genomics* 8: 131, 2007.
- Miao F, Wu X, Zhang L, Yuan YC, Riggs AD and Natarajan R: Genome-wide analysis of histone lysine methylation variations caused by diabetic conditions in human monocytes. *J Biol Chem* 282: 13854-13863, 2007.
- Zhang L, Dai Y, Wang L, Peng W, Zhang Y, Ou Y and Lu J: CpG array analysis of histone H3 lysine 4 trimethylation in peripheral blood mononuclear cells of uremia patients. *DNA Cell Biol* 30: 179-186, 2011.
- Gulbins E, Coggeshall KM, Brenner B, Schlottmann K, Linderkamp O and Lang F: Fas-induced apoptosis is mediated by activation of a Ras and Rac protein-regulated signaling pathway. *J Biol Chem* 271: 26389-26394, 1996.

19. Esteve P, Embade N, Perona R, Jiménez B, del Peso L, León J, Arends M, Miki T and Lacal JC: Rho-regulated signals induce apoptosis in vitro and in vivo by a p53-independent, but Bcl2 dependent pathway. *Oncogene* 17: 1855-1869, 1998.
20. Perletti L, Talarico D, Trecca D, Ronchetti D, Fracchiolla NS, Maiolo AT and Neri A: Identification of a novel gene, PSD, adjacent to NFKB2/lyt-10, which contains Sec7 and pleckstrin-homology domains. *Genomics* 46: 251-259, 1997.
21. Okada S, Suzuki K, Takaharu K, Noda H, Kamiyama H, Maeda T, Saito M, Koizumi K, Miyaki Y and Konishi F: Aberrant methylation of the pleckstrin and Sec7 domain-containing gene is implicated in ulcerative colitis-associated carcinogenesis through its inhibitory effect on apoptosis. *Int J Oncol* 40: 686-694, 2012.
22. Kang H, Cui K and Zhao K: BRG1 controls the activity of the retinoblastoma protein via regulation of p21^{CIP1/WAF1/SD1}. *Mol Cell Biol* 24: 1188-1199, 2004.
23. Zhang HS, Gavin M, Dahiya A, Postigo AA, Ma D, Luo RX, Harbour JW and Dean DC: Exit from G1 and S phase of the cell cycle is regulated by repressor complexes containing HDAC-Rb-hSWI/SNF and Rb-hSWI/SNF. *Cell* 101: 79-89, 2000.
24. Maitra A, Wistuba II, Washington C, Virmani AK, Ashfaq R, Milchgrub S, Gazdar AF and Minna JD: High-resolution chromosome 3p allelotyping of breast carcinomas and precursor lesions demonstrates frequent loss of heterozygosity and a discontinuous pattern of allele loss. *Am J Pathol* 159: 119-130, 2001.
25. Wistuba II, Gazdar AF and Minna JD: Molecular genetics of small cell lung carcinoma. *Semin Oncol* 28 (Suppl 4): 3-13, 2001.
26. DelBove J, Rosson G, Strobeck M, *et al*: Identification of a core member of the SWI/SNF complex, BAF155/SMARCC1, as a human tumor suppressor gene. *Epigenetics* 6: 1444-1453, 2011.
27. Xu Z, Liang L, Wang H, Li T and Zhao M: HCRP1, a novel gene that is downregulated in hepatocellular carcinoma, encodes a growth-inhibitory protein. *Biochem Biophys Res Commun* 311: 1057-1066, 2003.
28. Wittinger M, Vanhara P, El-Gazzar A, *et al*: hVps37A status affects prognosis and cetuximab sensitivity in ovarian cancer. *Clin Cancer Res* 17: 7816-7827, 2011.
29. Chang X, Li Z, Ma J, Deng P, Zhang S, Zhi Y, Chen J and Dai D: DNA methylation of NDRG2 in gastric cancer and its clinical significance. *Dig Dis Sci* 58: 715-723, 2013.
30. Zhi Y, Chen J, Zhang S, Chang X, Ma J and Dai D: Down-regulation of CXCL12 by DNA hypermethylation and its involvement in gastric cancer metastatic progression. *Dig Dis Sci* 57: 650-659, 2012.